

Binder Fiber Distribution and Tensile Properties of Thermally Point Bonded Cotton-Based Nonwovens

Haoming Rong, Gajanan S. Bhat

University of Tennessee, Knoxville, Tennessee 37996

Received 10 February 2003; accepted 1 August 2003

ABSTRACT: Cotton-based nonwovens are generally produced by carding and then bonding. One of the most important characteristics of nonwoven materials is the uniformity of their structure and properties. However, the carded webs always have irregularities caused by processing and material variables. The binder fiber distribution in carded cotton-based nonwoven fabrics was analyzed based on the crystallization behavior of one of the components of the binder fibers by DSC. The effects of process parameters, such as bonding temperature and binder fiber component, on the uniformity were discussed in detail in this article.

Also, the relationship of binder fiber distribution and the strip tensile property and single-bond tensile strength were investigated. The results showed that if the binder fibers were not well distributed in the fabric, it would be hard to get the same trend of temperature effect on tensile property for the strip and single-bond tests. © 2004 Wiley Periodicals, Inc. *J Appl Polym Sci* 91: 3148–3155, 2004

Key words: nonwovens; thermal calendaring; differential scanning calorimetry (DSC); specific heat; bicomponent binder fiber

INTRODUCTION

Carding is the most common process used to produce nonwoven fabrics from staple fibers. The objective of carding is to disentangle the fiber stock into individual fibers with minimum fiber breakage. Thus the carding process consists of opening and thoroughly blending different species of fibers. For cotton-based thermally point bonded nonwovens, it is important that the low-melting binder fiber be distributed evenly throughout to ensure uniformity of fabric properties. However, the carded webs always have area irregularities of mass distribution caused by machine variables (the nature and conditions of card clothing, the relative speeds and settings of the carding elements), fiber properties, and area irregularities of the fed fiber mat.¹ For any application, the most important characteristic of a carded web is uniformity of fiber areal density.

The mechanical properties of nonwoven fabrics depend on three groups of variables: the mechanical properties of the constituent fibers, which are the principal load carrying elements; the arrangement of the fibers in the web, which principally determines the web anisotropy, and the bonds that bind the fibers and transfer stresses.² Because strength is an extrinsic property, if some parts of a whole fabric sample are weakly bonded, such as regions with low binder fiber distribution, they may affect fabric strength significantly.

Although binder fiber distribution can be qualitatively determined by either dyeing the binder fiber, then observing the fabrics under microscopy, or by observing the different shapes of binder fiber under scanning electronic microscopy (SEM), there is hardly any report on any method used to quantitatively characterize the binder fiber distribution of the carded webs. Differential scanning calorimetry (DSC) can be used to measure the heat flow to and from the sample as a function of temperature. Various materials characteristics can be determined from these data, including oxidative stability, purity, and polymorphism. Chemical reactions, melting behavior, and the temperature evolution of the specific heat can also be investigated.^{3–5} In this article, DSC was used to determine the weight/weight concentration of the binder fiber in the thermally point bonded carded webs. Thus, the uniformity of the binder fiber distribution of the carded webs was evaluated by taking several measurements of specific enthalpy of cooling across the width of the web.

The objective of this study was to investigate the effect of binder fiber distribution on the mechanical properties of thermally bonded cotton-based nonwoven fabrics.

EXPERIMENTAL

Fibers

The fibers used in this study were cotton fiber, polyethylene/poly(ethylene terephthalate) (PE/PET) bicomponent binder fiber, and Eastar/polypropylene (PP) bicomponent binder fiber. The cotton fiber was supplied by Cotton Incorporated (Raleigh, NC). The

Correspondence to: H. Rong (hrong@utk.edu).

TABLE I
Properties of Selected Fibers (Single Filament)

Property	Cotton	PE/PET	Eastar/PP
Filament density (g/cm ³)	1.5	1.38	1.1
Filament tex (tex)	0.244	0.333	0.444
Peak strength (mN/tex)	152.2	264.8	269.6
Peak extension (%)	5.4	42.9	96.0
Initial modulus (mN/tex)	360.9	—	392.5
Staple length (in.)	0.96 ^a	1.5	1.5

^a Upper-half-mean fiber length.

scoured and bleached commodity cotton fiber had a moisture content of 5.2%, a micronaire value of 5.4, and an upper-half-mean fiber length of 24.4 mm (0.96 in.). The PE/PET bicomponent binder fiber was provided by Kosa, Inc. (Kingsport, TN). The Eastar *Bio* GP copolyester bicomponent (Eastar/PP) staple fibers were produced by Eastman Chemical Co. (Kingsport, TN). Both the bicomponent fibers have a sheath/core structure, with PE and Eastar *Bio* GP copolyester as the sheaths, and PET and PP as the stiffer cores. Properties of the three different fibers are listed in Table I. The two binder fibers have similar peak strength values, but Eastar/PP has an extension value twice that of PE/PET.

Nonwoven web processing procedures

The important steps in processing are shown in Figure 1. Fibers were first opened by hand and then weighed according to the desired blend ratio and fabric weight. The blend of fiber was then carded to form a web using a modified Hollingsworth card. The resulting carded fabric weights were about 40 g/m². The carded webs were then thermally point-bonded using a Ramisch Kleinewefers 60 cm (23.6 in.) wide calender with a bonded area of 16.6%. Three blend ratios (85/15, 70/30, and 50/50 of cotton/binder fiber), and two sets of calendering temperatures (100, 110, and 120°C; and 120, 130, and 140°C) were used for cotton/(Eastar/PP) series and cotton/(PE/PET) series, respectively. All the webs were calendered under the same nip pressure (0.33 MPa) at a constant speed of 10 m/min.

Characterizations

Tensile properties

The tensile properties of single-filament and nonwoven fabrics were tested using a united tensile tester according to ASTM D 3822-91 (Standard Test Method for Testing for Fiber/Filament) and ASTM D 1117-80 (Standard Test Method for Tensile Testing of Nonwoven Fabrics), respectively. All the tensile tests were carried out under the standard atmosphere for testing

textiles, with temperature of $21 \pm 1^\circ\text{C}$ and relative humidity of $65 \pm 2\%$.

Fabric weight

Basis weights of nonwoven fabrics were determined according to INDA Standard Test 130.1-92 (Standard Test Method for the Mass Per Unit Area of Nonwoven Fabrics).

Thermal analysis

The thermal properties of all the samples were analyzed using a Mettler differential scanning calorimeter (Model DSC-821, Mettler, Greifensee, Switzerland). Temperature calibration was performed using indium with the melting temperature of 156.56°C and heat of fusion (ΔH_f) of 28.54 J/g . To eliminate the effect of different heat histories of the two binder fibers during processing, the crystallization behavior of one of the binder fiber components was measured. For the cotton and PE/PET binder fiber series, the crystallization behavior of PE was measured. Samples ($\sim 5 \text{ mg}$) were first heated under nitrogen atmosphere (at a flow rate of 200 mL/min) at 150°C for 10 min to make sure the PE component of the binder fiber was fully melted, and then cooled to 50°C at a cooling rate of 10°C/min , whereas for the cotton and Eastar/PP binder fiber series, the crystallization behavior of PP was recorded. Samples ($\sim 5 \text{ mg}$) were first heated under a nitrogen atmosphere (at a flow rate of 200 mL/min) at 180°C for 10 min to make sure the PP component of the binder fiber was fully melted, and then cooled to 50°C at a cooling rate of 10°C/min .

The weight/weight concentration of the samples was obtained by calculating the ratio of the specific enthalpy of cooling for a certain web with the specific enthalpy of cooling for 100% binder fiber.

RESULTS AND DISCUSSION

Evaluation of DSC characterization method

To evaluate the accuracy of DSC measurement, first binder fiber and cotton fiber were manually blended

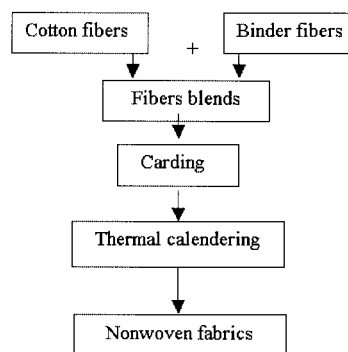


Figure 1 Flow chart of nonwoven web processing procedures.

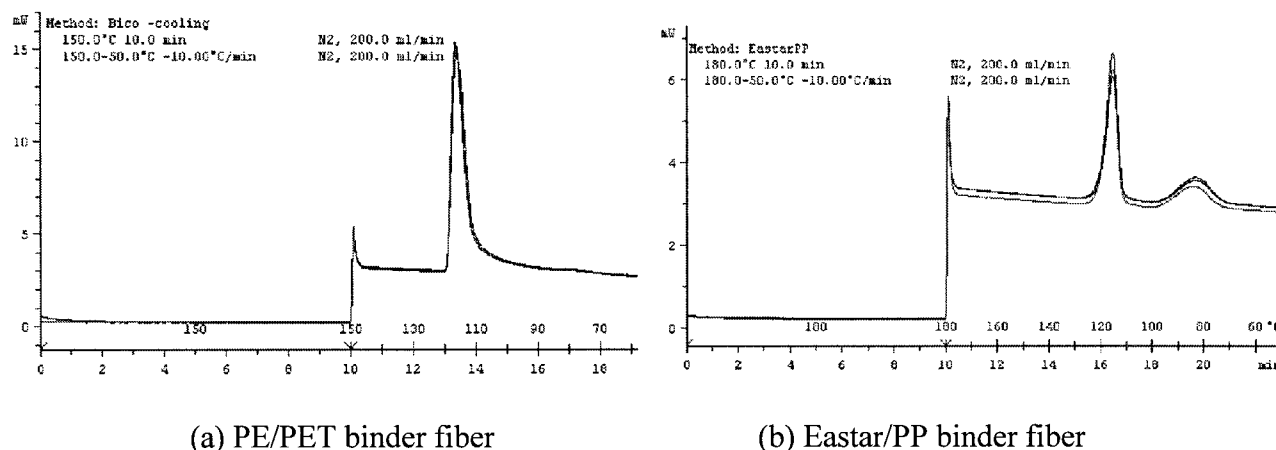


Figure 2 DSC traces of 100% binder fibers.

at different weight percentages, that is, binder fiber component of 100, 50, 40, 30, 20, and 10%. Each of the components was studied at least three times under the same conditions so that the standard deviation (σ) and the coefficient of variation (C.V.) could be measured. Figure 2(a) and (b) illustrates the DSC traces of 100% component of the two binder fibers.

Specific heat ($\Delta H/g$) values for the samples with 100% binder fibers were considered here as "Actual" as well as "Observed" for the sake of calculation. Subsequently, the "Observed" specific heats for the other components were calculated by the areas under the DSC exothermic peaks. Any error that occurred will be overcome by the conversion factor of gram (1000 mg) because the sample is taken at the milligram level for the DSC study. Then the "Observed" weight/weight concentration of the samples can be obtained

by calculating the ratio of the specific heat at a certain component with the specific heat for 100% binder fiber. Parameters obtained from the DSC measurements for the two different binder fiber series are summarized in Tables II and III.

Because PE is the only component melted and crystallized during the measurement of cotton/(PE/PET) blends, there is no obvious effect of cotton component on the crystallization behavior of PE. This can be verified by the near constant onset crystallization temperatures and the peak crystallization temperatures under different PE/PET components in Table II. In the case of cotton/(Eastar/PP) blends, although both the components (Eastar and PP) in the binder fiber melted and crystallized, the presence of the Eastar component has no significant effect on the primary nucleation and crystallization of the PP component because the onset

TABLE II
Parameters Obtained from DSC Measurements for Cotton/(PE/PET) Blends^a

"Actual" PE/PET (%)	$T_{o,c} = T_c$ (°C)	$T_{p,c}$ (°C)	ΔH_c (J/g)	Average ΔH_c (J/g)	σ (ΔH_c)	C.V.	"Observed" PE/PET (%)
100	119.17	116.75	89.49	90.20	2.241	0.025	100
	119.14	117.11	92.71				
	119.15	117.28	88.40				
50	118.93	117.32	44.46	44.23	0.854	0.019	49.04
	119.04	117.30	43.28				
	118.93	117.26	44.94				
40	118.95	117.23	36.89	35.80	1.047	0.029	39.69
	118.71	117.06	34.80				
	118.73	117.05	35.72				
30	118.64	117.06	26.50	26.31	0.219	0.008	29.17
	118.69	117.05	26.07				
	118.55	117.04	26.36				
20	118.66	116.96	17.66	17.42	0.216	0.012	19.31
	118.78	117.12	17.24				
	118.69	116.39	17.36				
10	118.26	116.53	8.38	8.31	0.110	0.013	9.21
	118.08	116.18	8.36				
	118.29	116.39	8.18				

^a T , temperature; c , cooling or crystallizing; o , onset; p , peak; ΔH_c , the specific enthalpy for PE exothermic peak.

TABLE III
Parameters Obtained from DSC Measurements for Cotton/(Eastar/PP) Blends^a

“Actual” Eastar/PP (%)	$T_{o,c} = T_c$ (°C)	$T_{p,c}$ (°C)	ΔH_c (J/g)	Average ΔH_c (J/g)	σ (ΔH_c)	C.V.	“Observed” Eastar/PP (%)
100	121.69	116.68	28.09	27.95	0.997	0.036	100
	122.77	117.10	26.89				
	122.10	116.61	28.87				
50	123.28	117.86	13.20	13.69	0.595	0.043	48.98
	122.41	117.03	13.51				
	122.07	116.67	14.35				
40	121.81	116.68	11.39	11.15	0.490	0.044	39.89
	121.67	115.83	10.59				
	121.57	115.82	11.48				
30	121.51	116.00	8.34	8.33	0.38	0.046	29.79
	121.77	116.83	7.94				
	122.15	117.32	8.70				
20	121.83	117.30	6.13	5.70	0.373	0.065	20.39
	122.55	117.46	5.54				
	122.79	117.62	5.44				
10	121.93	117.18	2.66	2.81	0.216	0.077	10.05
	120.47	115.44	3.06				
	121.71	116.76	2.72				

^a T , temperature; c , cooling or crystallizing; o , onset; p , peak; ΔH_c , the specific enthalpy for PP exothermic peak.

and peak crystallization temperatures of PP are almost stable for different Eastar/PP components of cotton/(Eastar/PP) blends (Table III). Therefore, there is no miscibility problem for both blend series. According to the data in Tables II and III, the “observed” binder fiber components are well fitted with the “actual” binder fiber components, with a variation of $\pm 1\%$.

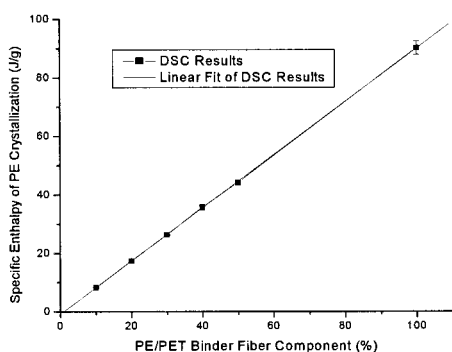
Results of the DSC measurements of specific enthalpy (ΔH_c) versus binder fiber weight concentration for the two binder fiber series are plotted in Figure 3(a) and (b). The regression lines fit both the binder fibers perfectly with regression coefficients of 0.99997 and 0.99987 for PE/PET binder fiber and Eastar/PP binder fiber, respectively.

Based on the preceding analysis, it appears that DSC specific enthalpy from crystallization of one of the binder fiber components in the cotton/binder blend series can be used to estimate binder fiber components in the samples.

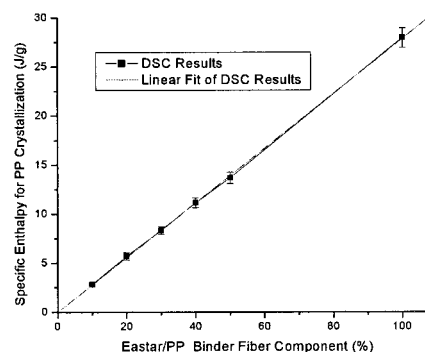
Binder fiber distribution of carded nonwovens

To describe the binder distribution in the web, five different positions along the cross-direction were selected (as shown in Fig. 4) at each binder component. Parameters obtained from the DSC measurements for the two different carded nonwoven fabric series are summarized in Tables IV and V.

It may be observed from the data in Tables IV and V that, although the “observed” average binder fiber content is close to the “actual” binder fiber content along the cross direction for both the nonwoven series, high variation and C.V. of the binder fiber component existed in some of the webs for both the carded nonwoven series. Therefore, we can say that binder fibers were not well distributed in those nonwoven fabrics. Apparently, the variation is much higher for the nonwovens of lower(est) binder fiber component.



(a) PE/PET binder fiber



(b) Eastar/PP binder fiber

Figure 3 DSC measured enthalpy versus binder fiber weight component.



Figure 4 Schematic illustration of sample selection for nonwoven fabrics.

Effect of binder fiber component on peak load of cotton-based nonwovens

The effect of bonding temperature under different binder fiber components on fabric peak load along the machine direction (MD) can be seen from the data in Figure 5(a) and (b). It can be clearly seen that with the increase in binder fiber component, peak load increases at all the bonding temperatures. This is the result of the increase of binder fiber, which causes an increase in the number of bond points and the effective bond area.

With an increase in thermal bonding temperature, the peak load first increases and then decreases at higher bonding temperatures. The first increase in strength of the fabrics is the result of the formation of a better-developed bonding structure. This can be verified by observing the SEM micrographs of the bond points (Fig. 6). The regular shape of the bonding points and smooth surface of the fabrics bonded at relatively high bonding temperature show the well-developed bond structure. However, with a further increase in bonding temperature the peak load decreases. This may be caused by a different failure mechanism of the fabrics bonded at higher temperatures.⁶

Failure of nonwoven fabrics can occur by failure of the fiber (fiber breakage), failure within the bond (adhesive breakage or cohesive failure) or at the fiber-binder bonding interface, or by a combination of these

TABLE IV
Parameters Obtained from DSC Measurements for Cotton/(PE/PET) Nonwovens^a

"Actual" PE/PET (%)	$T_{o,c} = T_c$ (°C)	$T_{p,c}$ (°C)	ΔH_c (J/g)	"Observed" PE/PET (%)	Average PE/PET (%)	σ	C.V.
50	118.84	117.24	59.00	65.41	51.83	11.9	0.230
	118.82	117.15	52.45	58.15			
	118.80	117.28	42.29	46.88			
	118.68	116.92	49.17	54.51			
	118.64	116.83	30.86	34.21			
30	118.71	117.19	28.23	31.30	27.85	7.02	0.252
	118.68	117.17	26.82	29.73			
	118.73	117.21	33.15	36.75			
	118.49	116.94	18.00	19.96			
	118.58	116.94	19.40	21.51			
15	118.65	117.01	20.63	22.87	14.42	6.64	0.460
	118.46	116.82	17.82	19.76			
	118.40	116.87	6.87	7.62			
	118.56	117.06	11.37	12.61			
	118.51	117.01	8.33	9.24			

^a "Actual" PE/PET (%) is the input % for the carding process; T , temperature; c , cooling or crystallizing; o , onset; p , peak; ΔH_c , the specific enthalpy for PE exothermic peak.

TABLE V
Parameters Obtained from DSC Measurements for Cotton/(Eastar/PP) Nonwovens^a

"Actual" Eastar/PP (%)	$T_{o,c} = T_c$ (°C)	$T_{p,c}$ (°C)	ΔH_c (J/g)	"Observed" Eastar/PP (%)	Average Eastar/PP (%)	σ	C.V.
50	121.50	117.06	13.87	49.62	47.52	3.97	0.083
	121.33	116.88	13.98	50.02			
	121.14	116.71	14.26	51.02			
	121.23	116.31	12.65	45.26			
	120.64	115.95	11.65	41.68			
30	120.71	116.52	10.67	38.18	31.09	4.61	0.148
	120.65	116.50	7.60	27.19			
	121.27	116.84	8.55	30.59			
	120.21	116.29	7.53	26.94			
	120.74	116.62	9.10	32.56			
15	123.02	118.80	5.47	19.57	13.98	4.81	0.344
	123.16	119.13	4.35	15.56			
	122.89	118.79	3.30	11.81			
	122.93	118.75	4.48	16.03			
	122.99	118.89	1.93	6.91			

^a "Actual" Eastar/PP (%) is the input % for the carding process T , temperature; c , cooling or crystallizing; o , onset; p , peak; ΔH_c , the specific enthalpy for PP exothermic peak.

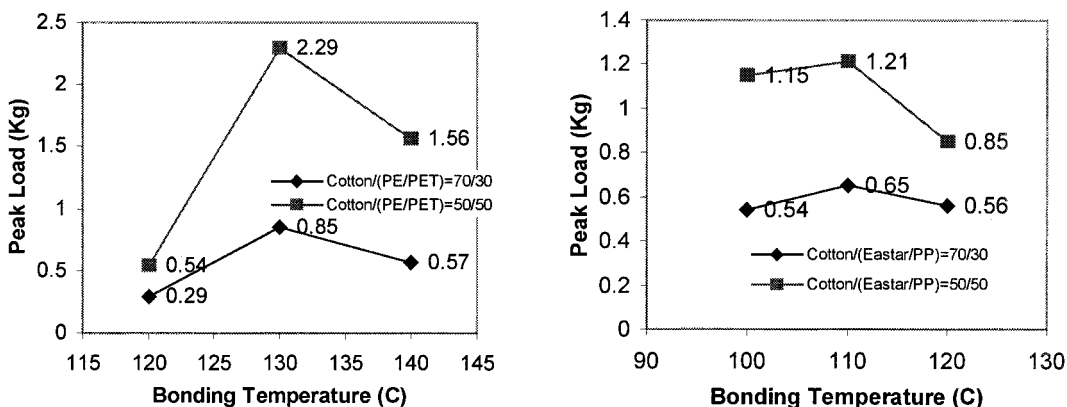


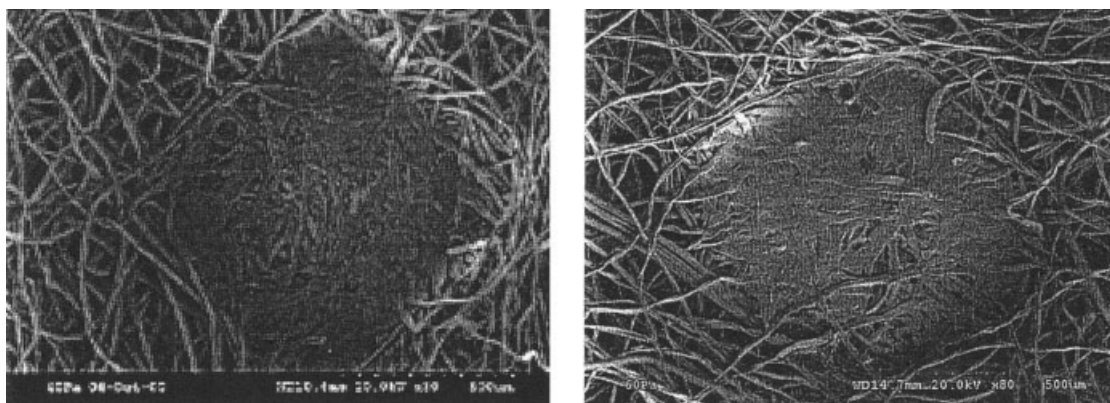
Figure 5 Effect of bonding temperature on peak load of cotton-based nonwovens (machine direction). Fabric weight: about 40 g/m²; calendering pressure: 0.33 MPa; calendering speed: 10 m/min.

modes. The interaction of component properties, structure, and fabric deformation mechanisms can lead to a variety of unique failure mechanisms for nonwoven fabrics. The nonwoven fabric failure mechanism is influenced by fiber physical properties, adhesive properties, and structural properties including the relative frequency and structure of the bonding elements, fiber orientation, and the degree of liberty of movement of the fibers between the bond points. Physical properties of the nonwoven fabrics will be controlled by the first failure occurring in the fabric sample.⁷ We can say that the failure mechanism of nonwoven fabrics bonded at higher temperature is different from that of the nonwoven fabrics bonded at a lower calendering temperature. This difference in failure mechanism can be confirmed by the SEM micrographs of the failure structures of the fabrics produced at different bonding temperatures (Fig. 7).

These observations are consistent with those of Gibson and McGill,⁸ who studied the failure mechanism of thermally point bonded polyester nonwovens as a function of bonding temperature. At low bonding temperatures, the bond failure mechanism was found to be attributed to loss of interfacial adhesion at the bond site leading to bond disintegration. At higher bonding temperatures, the failure mechanism was cohesive failure of the fibers near the bond site attachment point. Similar observations were made with PP thermally bonded and spunbonded nonwovens by Bhat et al.^{9,10}

Single bond strip tensile test results of the cotton-based nonwoven fabrics

To further analyze the effect of binder fiber distribution on fabric strength, a single-bond strip tensile test



(a) Cotton/(PE/PET): 70/30
 Bonding Temperature: 130°C
 Calendering Pressure: 0.33MPa
 Calendering speed: 10m/min
 Fabric weight: ~ 40g/m²

(b) Cotton/(Eastar/PP): 70/30
 Bonding Temperature: 110°C
 Calendering Pressure: 0.33MPa
 Calendering speed: 10m/min
 Fabric weight: ~ 40g/m²

Figure 6 SEM micrographs of cotton-based nonwoven fabrics.

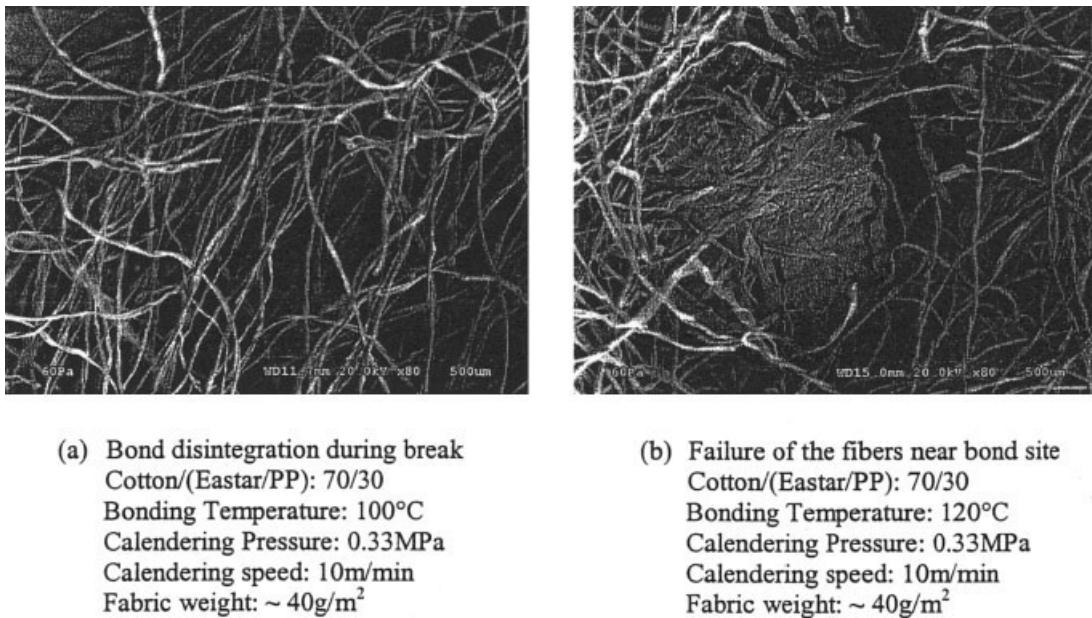


Figure 7 SEM micrographs of failure structure after tensile testing for cotton/(Easter/PP) nonwoven fabrics (machine direction).

was carried out for the two cotton-based nonwoven fabrics series. This test was done to estimate the bond strength and the degree of load sharing between fibers during the tensile deformation of the web. A schematic of this test is shown in Figure 8. A strip of size 80×5 mm was cut from the web. The strip was cut across the width direction from the two sides to leave only one bond uncut in the middle of the strip. The strip was then subjected to a conventional tensile test. The test was conducted on the United Tensile Tester with a gauge length of 1 in. (2.54 cm) and extension rate of 0.5 in./min (1.27 cm/min). A total of 20 tests were done for each sample.

Results of the single-bond strip tensile test for the two binder fiber series are shown in Figure 9(a) and (b). If the binder fibers were well distributed in the

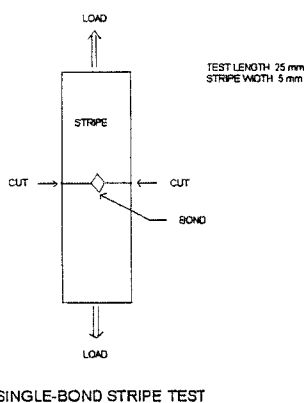


Figure 8 Schematic illustration of single-bond strip tensile test.

nonwoven fabrics, the effect of bonding temperature on the tensile strength of strip fabrics should be consistent with that of the single-bond strips.

Comparing Figure 9 with Figure 5, we can see that the trends of the peak load data in the two figures are not exactly the same. In the case of cotton/(PE/PET) nonwovens, at a binder fiber component of 30%, the trend of the curve for the strip test is the same as that for the single-bond strip test, whereas for the binder fiber component of 50%, the trend of the peak load for the strip test does not follow the same trend as that of the single-bond strip test. This is the result of the high variation of binder fiber distribution along the cross-direction of the fabric. The standard deviation of the fabric with 50% PE/PET binder fiber is 11.90, listed in Table IV, which is much higher than that of the fabric with 30% PE/PET binder fiber (7.02), although the C.V. values of the two fabrics are close to each other.

However, in the case of cotton/(Easter/PP) nonwovens, at the binder fiber component of 50%, the trend of the peak load for the strip test is the same as that for the single-bond strip test, whereas for the binder fiber component of 30%, the trend of the peak load for the strip test does not follow the same trend as that of the single-bond strip test. Again, it is the result of the high variation of binder fiber distribution along the cross-direction of the fabric with binder fiber component of 30%. The C.V. and standard deviation of the fabric with 30% Easter/PP binder fiber are 14.8% and 4.61, respectively, listed in Table V, which are higher than those of the fabric with 50% Easter/PP binder fiber, which are 8.3% and 3.94, respectively.

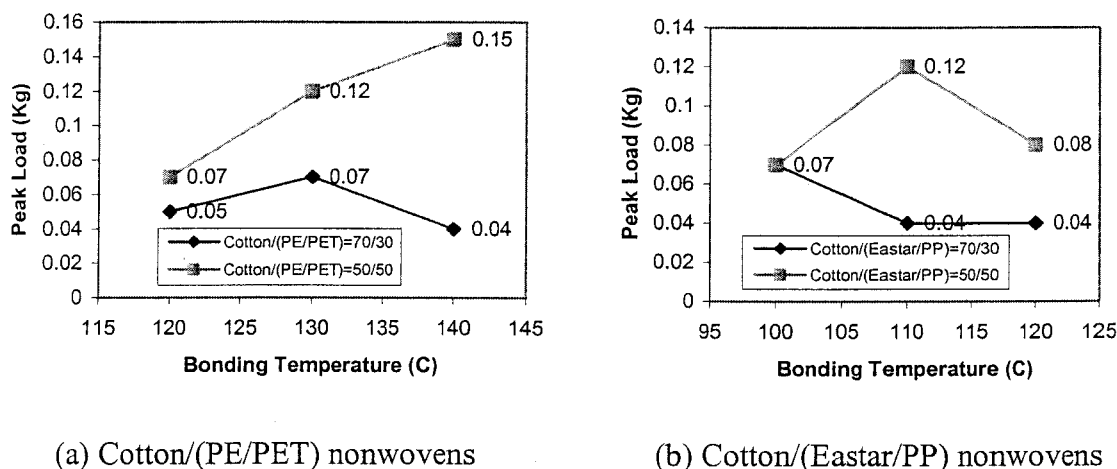


Figure 9 Effect of bonding temperature on peak load of single-bond strips (machine direction). Fabric weight: about 40 g/m²; calendering pressure: 0.33 MPa; calendering speed: 10 m/min.

CONCLUSIONS

The results show that DSC is a useful and a reliable method for studying the binder fiber distribution in the carded cotton-based nonwovens by analyzing the specific enthalpy from crystallization of one of the binder fiber components in the fabrics. Because a high standard deviation and C.V. of the binder fiber component existed in both of the carded nonwoven series according to DSC measurement results, we can conclude that binder fibers were not well distributed in those nonwoven fabrics series. This result is consistent with the comparison of tensile test results of fabric strips and single-bond strips. If the binder fibers were well distributed in the nonwoven fabrics, the effect of bonding temperature on the tensile property of strip fabric should be consistent with that of the single bond strip. In fact, the trends of the tensile curves under different bonding temperatures for the two binder fiber series are not exactly the same. This further verified that binder fibers were not well distributed on those carded nonwoven fabrics, especially for certain compositions.

Binder fiber component and bonding temperature are the two main variables that determine the properties of final thermal bonding nonwoven products. With the increase of binder fiber component, the peak load increases. With the increase of bonding temperature, the peak load first increases and then decreases with further bonding temperature increase. The initial

increase in strength of the fabrics is the result of the formation of a better-developed bonding structure. The further decrease of peak load may be caused by the different failure mechanism of the fabrics bonded at higher temperature.

The authors thank Cotton Incorporated, Raleigh, NC and Tennessee Agricultural Experimental Station for the financial support; and Kosa Inc. and Eastman Chemical Company, Kingsport, TN for providing binder fibers for this study.

References

- Meng, J.; Seyam, A. M.; Batra, S. K. *Text Res J* 1999, 69, 90.
- Erel, S.; Warner, S. B. *Text Res J* 2001, 71, 22.
- Pagella, C.; De Faveri D. M. *Prog Org Coat* 1998, 33, 211.
- Zhao, M.; Shen, B.; Liu, F. In: *Analysis of Paraffin Wax Fraction in Asphalt by DSC*, Proceedings of the International Symposium on Heavy Oil and Residue Upgrading and Utilization, 1992; pp. 63–65.
- Tripathy, A. R.; Patra, P. K.; Sinha, J. K.; Banerji, M. S. *J Appl Polym Sci* 2002, 83, 937.
- Rong, H.; Bhat, G. S. *Int Nonwovens J* 2003, 12, 53.
- Hansen, S. M. *Nonwoven Engineering Principles: Nonwovens—Theory, Process, Performance, and Testing*; Turbak, A. F., Ed.; TAPPI Press: Atlanta, GA, 1993; Chapter 5.
- Gibson, P. E.; McGill, R. L. In: *Proceedings of the 1987 TAPPI Nonwovens Conference*; TAPPI Press: Atlanta, GA, 1987; p. 129.
- Bhat, G. S.; Kotra, R.; Nanjundappa, R.; In *Proceedings of INTC 2001*, September 5–7, 2001, Baltimore, MD.
- Bhat, G. S.; Chand, S.; Spruiell, J. E.; Malkan, S. R. *Thermochim Acta* 2001, 367/368, 155.